

Review

Terrestrial Remotely Sensed Imagery in Support of Public Health: New Avenues of Research Using Object-Based Image Analysis

Maggi Kelly ^{1,2,*}, Samuel D. Blanchard ¹, Ellen Kersten ¹ and Kevin Koy ²

¹ Department of Environmental Science, Policy and Management, University of California, Berkeley, 130 Mulford Hall #3114, Berkeley, CA 94720, USA; E-Mails: sablanchar@berkeley.edu (S.B.); ekersten@berkeley.edu (E.K.)

² Geospatial Innovation Facility, College of Natural Resources, University of California, Berkeley, Berkeley, CA 94720, USA; E-Mail: kkoy@berkeley.edu

* Author to whom correspondence should be addressed; E-Mail: maggi@berkeley.edu.

Received: 15 August 2011; in revised form: 7 October 2011 / Accepted: 20 October 2011 /

Published: 27 October 2011

Abstract: The benefits of terrestrial remote sensing in the environmental sciences are clear across a range of applications, and increasingly remote sensing analyses are being integrated into public health research. This integration has largely been in two areas: first, through the inclusion of continuous remote sensing products such as normalized difference vegetation index (NDVI) or moisture indices to answer large-area questions associated with the epidemiology of vector-borne diseases or other health exposures; and second, through image classification to map discrete landscape patches that provide habitat to disease-vectors or that promote poor health. In this second arena, new improvements in object-based image analysis (or “OBIA”) can provide advantages for public health research. Rather than classifying each pixel based on its spectral content alone, the OBIA approach first segments an image into objects, or segments, based on spatially connected pixels with similar spectral properties, and then these objects are classified based on their spectral, spatial and contextual attributes as well as by their interrelations across scales. The approach can lead to increases in classification accuracy, and it can also develop multi-scale topologies between objects that can be utilized to help understand human-disease-health systems. This paper provides a brief review of what has been done in the public health literature with continuous and discrete mapping, and then highlights the key concepts in OBIA that could be more of use to public health researchers interested in integrating remote sensing into their work.

Keywords: object-based image analysis (OBIA); vector-borne diseases; health exposures; image classification; fine spatial resolution imagery; topology

1. Introduction

The synoptic, multi-spectral and multi-temporal coverage provided by terrestrial remote sensing programs has been a boon to a range of environmental science applications, including terrestrial ecology [1], ecosystem characterization [2], disturbance [3-5], land use and land cover change [6-8], and biogeochemical cycling and ecosystem functioning [9-11], to name a few important avenues of research. The origins of these efforts were often contemporaneous with the development of national remote sensing programs such as Landsat (e.g., [12,13]). More recently, remote sensing analysis and products have begun to be integrated into public health research. Despite some skepticism (e.g., [14]) this is in large a positive trend, allowing for the examination of broad scale patterns in landscapes that may lead to or prevent spread of disease [15], delineation of habitat patches and refugia for disease vectors or their hosts [16-18], and the measurement of environmental and biophysical variables (e.g., temperature, amount and health of vegetation) for use in process-based models that capture human-animal disease dynamics and predict disease risk [18-20]. Remote sensing has been used to target sampling efforts and health interventions [21], and in the analysis of chemical and other exposures [16,22].

It is illuminating to discuss the contributions of remote sensing to the field of public health in light of two recent parallel trends in remote sensing: the first is the resurgence in production and use of field-based products best exemplified by normalized difference vegetation index (NDVI) [23,24], and by recent additions such as continuous percentage of tree cover (e.g., [25]) or continuous percentage of impervious surface cover [26,27]. These field-based, continuous data products derived from remotely sensed imagery are very useful in ecology: they capture inherent spatial gradients in the target being mapped (vegetation vigor, soil moisture, *etc.*) which vary over space, and they are commonly used in computational spatial models that are raster based and require control over cell size [28]. They are large-scale, economical, and anonymous [22], and they are in widespread use across environmental science, and are often included in epidemiological models [19,29].

Paralleling this development is the recent increase in object-based approaches for classification of fine (e.g., <5 m) and sometimes moderate (e.g., 10–30 m) spatial resolution imagery across multiple mapping domains [30]. It is increasingly acknowledged that pixel-based methods, while useful in classifying coarse-scale (>30 m) remotely sensed imagery, are less suitable for classifying fine spatial resolution images, such as those provided by digital aerial photographs and IKONOS and QuickBird satellites [31,32]. Pixel-based methods are less useful as they often result in image speckle and overall inaccuracies when applied to fine-resolution imagery (Figure 1). This is discussed more below. These object based image analysis (OBIA) methods are becoming more commonly used when the target being mapped has natural or clear discrete boundaries: patches, fields, houses, *etc.*, or when the pixel size in the imagery being analyzed is smaller than its target [30]. The OBIA approach first segments an image into image objects, or segments, which are defined as a group of spatially connected pixels with

similar spectral properties, and then these segments are classified based on their spectral and spatial attributes as well as by their interrelations across scales [31,33] (Figure 2). These kinds of multi-scaled patterns can be used to construct rules for classifying image objects and developing classification results in an OBIA framework, but they also convey important information about the resulting objects, which can be used to help understand how landscapes function and change. In the environmental sciences, such approaches have been used to understand how ecological features change through time under different management or climactic regimes [34-38]; how landscape pattern can impede or promote disease spread in a natural setting [39,40]; and can help guide management or restoration of landscapes [41,42]. Many of these concepts have their theoretical origins in landscape ecology.

Figure 1. Example of the speckle, or the “salt-and-pepper” effect common to pixel-based classifications of fine spatial resolution imagery: (a) an unsupervised classification of land cover from a suburban area in California; (b) the same area classified with an object-based classifier.

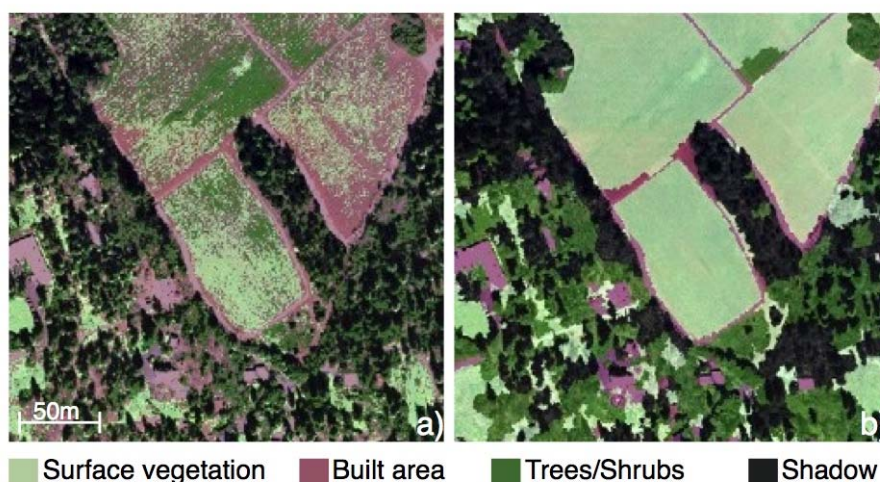
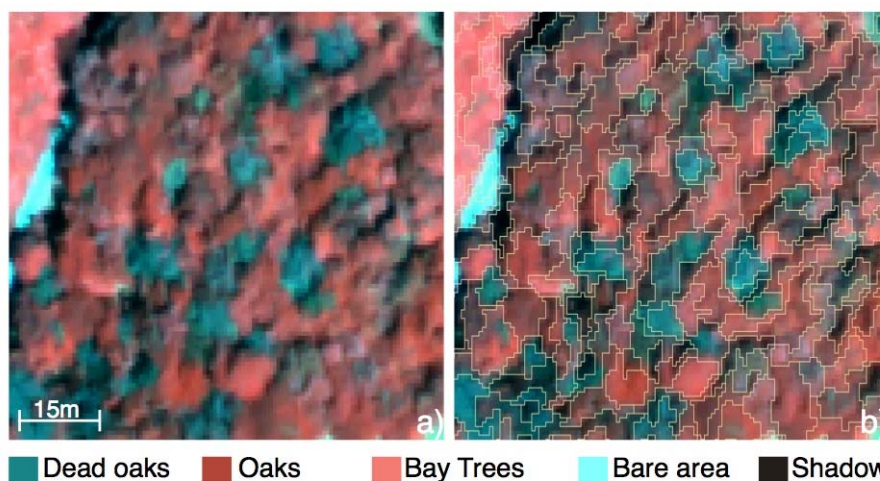


Figure 2. The first step of the OBIA process: the image segmentation process: (a) a fine spatial resolution color infrared image of an oak forest stand with dead trees; (b) the corresponding image segments. A 15m scale bar is present in panel (a).



Yet compared to the environmental sciences, there are relatively few examples of research in public health that use these OBIA approaches. One of the more recent exceptions is Maxwell [22], who provides a brief review of the use of remote sensing to map discrete landscape patches that can indirectly influence human health—either through the provision of habitat for a disease vector, or through a harmful land use practice—and a demonstration of OBIA to more accurately map land cover features at multiple scales over time to understand pesticide drift from agricultural fields. There are other examples (discussed below), but their relative paucity is interesting, since some of the key algorithms commonly used in geographic OBIA were developed for medical and health related applications. For example, the challenges faced by analysts examining microscopic images of biopsy samples [43,44], counting and classifying microbial colonies or cells on slides [45,46], or searching for pathological features in biological imaging applications (including laser-scanning microscopy and magnetic resonance imaging (MRI) technology) [47-49] all require the ability to extract meaningful objects from their image background, and use that information to support better diagnostics. Commercially available software commonly used in geographic OBIA applications, such as eCognition (previously known as Definiens' eCognition) [22,30,41,50,51] were influenced in their early development by such analysis of images from cell-based assays, whole tissue slides and full body scans [52,53], and indeed the two arenas, medical OBIA and geographic or environmental OBIA, continue to develop side-by-side with few interdisciplinary publication outlets. While it is the classification accuracy benefits to OBIA that are most often cited in the public health remote sensing literature [54,55], it is the ability of OBIA to capture fundamental spatial content across scales, and their interactions, that can be critical to understanding a system. This type of spatial content could be more frequently used in public health applications to understand complex systems and their interrelations.

This paper seeks to address the relative lack of use of OBIA in public health research, and provide a brief review of what has been done in the public health field with remote sensing, both with continuous and discrete mapping, and then highlight the key concepts in OBIA that could be useful to researchers in the public health arena. In this paper, we adopt a definition of public health similar to the World Health Organization, which states that health is a state of complete physical, mental and social well-being and not merely the absence of disease or infirmity. While many review papers are organized within a biological framework, investigating various disease categories (e.g., [14]), this paper will utilize a technological framework, and concentrate on the data products and formats themselves. We make a clear distinction between the analysis of continuous and discrete remotely sensed products for public health research. This review also positions OBIA for public health applications in a wider technological context than do other recent review papers on public health and OBIA (e.g., [22]).

2. The Use of Continuous Products in Public Health Research

Any discussion of the use of continuous products derived from remotely sensed imagery in public health applications should begin with an examination of the workhorse of the terrestrial remote sensing programs worldwide: NDVI [56-59]. NDVI is a measurement of vegetation abundance and vigor and is directly related to relative humidity and rainfall as well as to vegetation growth; it is often used as a proxy for, or to augment, measures of surface climatic conditions. And since bio-climatic conditions

are key determinants of arthropod vector distribution and abundance and consequently affect transmission rates of any diseases they may carry [60], NDVI is commonly used in models of vector suitability [61,62], abundance [20], and disease transmission and early warning [63,64]. The following research is summarized in Table 1.

Table 1. Summary of literature in public health using continuous data products.*

Remotely Sensed Data	Remotely Sensed Variables/Target	Location	Application (Disease/Condition)	Reference
Landsat	NDVI	Marion County, Indiana	Risk modeling (Obesity)	[65]
Landsat	NDVI	Seattle, Washington	Risk modeling (Obesity)	[66]
Landsat	NDVI	Southern California	Risk modeling (Obesity)	[67]
Landsat, NLCD	NDVI, Land cover	Southern California	Risk modeling (Obesity)	[68]
Landsat TM	Kauth-Thomas	Westchester County, New York	Vector-borne disease modeling (Lyme)	[69]
Landsat ETM+	NDVI	Marion County, Indiana	Risk modeling (Obesity)	[70]
Landsat MSS & TM, AVHRR	NDVI	Africa	Vector-borne disease modeling (Ebola Hemorrhagic Fever)	[71]
Landsat TM, NLCD	LST, Land cover	Philadelphia, Pennsylvania	Risk modeling (Extreme heat exposure)	[72]
MODIS, ASTER, QuickBird	EVI, NDVI, Land cover	Costa Rica	Vector-borne disease modeling (Dengue Fever)	[61]
MODIS	NDVI, LST	Uganda	Vector-borne disease modeling (Schistosoma)	[73]
AVHRR	Climate, NDVI	United States	Vector-borne disease modeling (Lyme)	[62]
AVHRR	LST	United States	Vector-borne disease modeling (West Nile Fever)	[63]
AVHRR, Meteosat	NDVI, CCD	Kenya	Vector-borne disease modeling (Malaria)	[74]
AVHRR, Meteosat	NDVI, CCD	Gambia	Vector-borne disease modeling (Malaria)	[75]
AVHRR, Meteosat	NDVI, LST, CCD	East Africa	Vector-borne disease modeling (Malaria)	[76]
AVHRR	NDVI, LST	Tanzania	Vector-borne disease modeling (Schistosomiasis)	[77]
AVHRR	Climate, NDVI	East Africa	Vector-borne disease modeling (Rift Valley Fever)	[78]
AVHRR	Climate, NDVI	East Africa	Vector-borne disease modeling (Rift Valley Fever)	[64]

*Note: NDVI: Normalized Difference Vegetation Index; EVI: Enhanced Vegetation Index; CCD: Cold-Cloud-Duration; LST: Land Surface Temperature; MODIS: Moderate Resolution Imaging Spectroradiometer; ASTER: Advanced Spaceborne Thermal Emission and Reflection Radiometer; AVHRR: Advanced Very High Resolution Radiometer; ETM: Enhanced Thematic Mapper; TM: Thematic Mapper; MSS: Multispectral Scanner System; NLCD: National Land Cover Database.

An early and important work by Rogers *et al.* [74] used terrestrial multispectral imagery combined with meteorological remotely sensed data (NOAA-AVHRR and Meteosat-HRR42). Land surface temperature, rainfall, cloud cover, middle infrared reflectance and NDVI were transformed with temporal Fourier processing and compared with the mean percentage of total annual malaria cases recorded each month at three sites in Kenya. The NDVI lagged by one month, and was found to be the most significant and consistently correlated variable with malaria admissions across the sites [75,76]. Hay *et al.* [75] continued this analysis in Gambia and found similar results with the exception that the cold cloud duration (CCD) was the best predictor of malaria cases. These and other similar work from related groups are summarized in Hay *et al.* [79].

Multi-temporal NDVI, when combined with land surface temperature measures across seasons, have proven to be a potent combination for vector-borne disease prediction. Models were developed using NDVI and temperature to map endemic areas and transmission potential of the disease schistosomiasis in China [20], and in Tanzania [77] and Uganda [73] in Africa. Anyamba and colleagues [78] used a 19-year NDVI time-series data derived from Advanced Very High Resolution Radiometer (AVHRR) to map areas with a potential for rift valley fever outbreak in east Africa. Rift valley fever risk was associated with NDVI anomalies in the time-series: they found a close agreement between confirmed outbreaks between 1981 and 2000 and these anomalies. Similar methods and results were found by Tucker and colleagues [71], who used AVHRR NDVI time-series data to examine Ebola hemorrhagic fever outbreaks in the 1970s and the 1990s in tropical Africa.

More recent and novel uses of continuous products like NDVI in public health focus on chronic diseases such as obesity. For example, Liu and colleagues [70] explored associations between risk for childhood overweight and two environmental factors: the amount of vegetation surrounding a child's residence and the proximity of the child's residence to various types of food retail locations. The amount of vegetation was obtained using Landsat ETM+ imagery transformed into NDVI. They found that after controlling for individual socio-demographics and neighborhood socioeconomic status, increased neighborhood vegetation was associated with decreased risk for overweight, but only for subjects residing in higher population density regions. Others have found similar results between higher greenness (as measured by NDVI) and lower body mass index (BMI) levels in children [65], and adults [66].

Continuous spatial data has also been used to create measures of neighborhood-level confounding variables to better identify the independent effects of particular health hazards and resources. For example, Jerrett and colleagues [67] used average NDVI within a 500 m buffer around each subject's residence as one of many confounding risk factors in models that identified a significant positive relationship between BMI and automobile traffic density around children's homes in southern California. Similarly, Wolch and colleagues [68] used image derivatives from the Landsat-based National Land Cover Database (NLCD) to create measures of average percent urban imperviousness and average percent tree canopy cover within 500 m buffers around each subject's residence. These measures, in addition to average NDVI and other neighborhood and individual-level factors, were included in models that demonstrate an inverse association between access to parks and recreational resources and increases in childhood BMI.

Alternatives to NDVI and NLCD derivatives include other vegetation image transformations such as Kauth-Thomas [80] wetness and greenness indices, which have successfully been used to map

risk for Lyme disease in the United States [18,69]. Other remotely sensed products are also useful in public health. Johnson and colleagues [72] investigated the complex spatial patterning of extreme heat events in urban environments by integrating sociodemographic risk factors with estimates of land surface temperature derived from thermal remote sensing data. They found they could better understand intra-urban variations in risk from extreme heat when remotely sensed estimates of land surface temperature were added to their risk model.

The aforementioned types of remotely sensed products and applications are not amenable to object-based image analysis. Gradients and regional scale spatial heterogeneity are what drive the models and dominate the results. However, there are areas where the ability to accurately map and delineate discrete landscape features via remote sensing are of importance to epidemiology and public health studies. These are primarily in mapping vector habitat and land use/land cover exposures.

3. Review of the Use of Discrete Products in Public Health Research

The potential of moderate spatial resolution remotely sensed images to map and measure the habitat for disease vectors and to enhance our understanding of the epidemiology and control of diseases was highlighted early (e.g., [81,82]), but the practice increased in the late 1990s [19], and continues to grow. The distribution of efficiently transmitted pathogens is generally limited by the distribution of vectors, whose habitats can sometimes be mapped with satellite imagery [83]. Kalluri and colleagues [15] provide a vector-specific review, and there are other literature surveys focusing on continents, e.g., Hay and colleagues [79] for mosquito-borne diseases in Africa; schistosomiasis in Africa [19] and in China [20,84]. For the most part these are positive assessments, highlighting the ability to map known habitats for subsequent surveillance, or to find novel habitats. For example, using Landsat TM and ETM+ imagery, Zou and colleagues [85] mapped potential habitats of the larvae of the mosquito *Culex tarsalis* (Coquillett), a main vector in the transmission of West Nile Virus in north central Wyoming, and found novel mosquito larval habitats in coal methane water sites in the study area. Seto and colleagues [86] used Landsat TM to map habitats suitable for *Oncomelania hupensis robertsoni* the snail vector responsible for schistosomiasis transmission in Sichuan, China. They used an unsupervised classification approach, and distinguished snail habitats from non-habitats in the mountainous regions of Sichuan.

But many scholars point out the mismatch between moderate scale imagery (e.g., Système Pour l'Observation de la Terre (SPOT) or Landsat) and the fine-scale habitat features that are not directly captured in such imagery. For example, Achee *et al.* [87] show that the preferred larval habitat of the mosquito *Anopheles darlingi* that spreads the *Plasmodium falciparum* infections between people and causes malaria in Belize is floating bamboo detritus patches along river margins. Their spatial analyses of SPOT satellite imagery found no associations between land cover and positive mosquito habitats. More promising, Mutuku *et al.* [88] show that IKONOS imagery was not useful in direct detection of small *Anopheles* larvae habitats in Kenya because of their size, but was useful in the localization of them through statistical association with specific land covers. Their classification of IKONOS yielded seven land cover classes, and agricultural land covers were found to be positively associated with presence of larval habitats, and were located relatively close to stream channels. Whereas

non-agricultural land covers were negatively associated with presence of larval habitats and were more distant from stream channels.

Remote sensing classification approaches are also used to elucidate the land covers and land uses that when proximate to a vulnerable population, can lead to disease. In this case, the most common approach is to use existing land cover and land use products, or to create new classification schemes, to map the habitat for a chemical exposure, such as pesticides. These maps are then used in subsequent analyses that model disease risk or highlight new insights in disease epidemiology. For instance, Brody [89] used land cover maps from Landsat ETM+ to estimate individual historical exposure levels to pesticides based on a number of spatial factors, including residential proximity to land cover classes most likely to contribute pesticide exposure and size of source area in Cape Cod, Massachusetts. Similarly, Landsat imagery was used by Ward *et al.* [90] to determine whether crop maps were useful for predicting residential levels of exposure to crop herbicides in Iowa. They concluded that satellite-based crop maps may be useful for estimating levels of herbicides in homes near crop fields, serving as a surrogate measure of potential exposure to agricultural pesticides [91].

Another common approach is to examine the relative proportion of land use/land cover classes that surround a feature of interest—a well, or household or a village—to determine if exposure, disease outcome or vector abundance can be linked to these contextual features. This approach is common in riparian studies [92] and requires mapping of land use/land cover classes as discrete polygons. An early example was Roberts *et al.* [93] who examined the proportion of mapped landscape elements surrounding 40 villages in Belize where data on malaria incidence had been collected. They used SPOT imagery and pixel-based classifiers to map the land use/land cover surrounding the villages. They found that the most important landscape elements in terms of explaining vector abundance in villages were transitional swamp and unmanaged pasture. Using a similar approach, but with a previously classified dataset, Ayotte *et al.* [16] hypothesized that increased bladder cancer risk was linked to elevated concentrations of inorganic arsenic in drinking water in New England, USA, and they examined characteristics in bedrock chemistry in addition to the land cover provided by the National Land Cover Data Set (NLCD) [94] in the area immediately surrounding each well for which arsenic data had been collected. Dambach *et al.* [95], who were investigating malaria risk in the lowlands of Burkina Faso, classified SPOT imagery into 10 land use/land cover classes using a supervised classification approach. The percentage of very high and high-risk land cover within a 500 m buffer zone of all villages (representing the assumed flying range of *Anopheles* mosquitos) was used to identify villages at risk for malaria. They present this work as a first step in targeting control measures in an area with endemic malaria.

Another important area of research involves the use of land use/land cover maps in subsequent landscape analysis. Landscapes are complex systems, displaying a dynamic interplay between structure (the spatial relationship among distinct elements or structural components of a system) and function (the productivity, nutrient cycling, animal movement and population dynamics of a system) [35,96,97]. In this landscape epidemiological view, disease occurrence can arise not just from the presence of a habitat, but from the underlying variations in these landscapes [54,98]. Land use/land cover maps have been used to examine the interplay between pattern and process across a range of environmental sciences. This is typically done through the use of landscape or pattern metrics, which explicitly capture spatial structure of patches, classes and landscapes [37,99-101]. Pattern metrics are calculated

using equations that quantify the spatial characteristics of individual patches, or a particular class within a landscape, and the spatial pattern of the landscape as a whole, using remotely sensed imagery as the input data [35]. Landscape metrics measure how patches are shaped, how they are distributed across the landscape, and how complex or simple a landscape is.

While these types of analyses of metrics are common in environmental sciences (e.g., [35,37]) and environmental management (e.g., [36]), they are still infrequent in public health. One example in the public health field is Liu and Weng [102] who examined landscape configuration and West Nile Virus incidence in Cook County, Illinois. They developed land use/land cover maps with six classes using an unsupervised classifier on Terra's Advanced Spaceborne Thermal Emission and Reflection Radiometer (ASTER) imagery. Landscape-level metrics were derived from their land use/land cover maps for the municipalities having mosquito/animal host positive reports. They found that the landscape factors, such as a landscape aggregation index and urban areas and areas of grass and water, showed strong correlations with the prevalence of West Nile Virus. Other examples come from Graham and colleagues [103,104] who have been examining the role of landscape pattern in transmission of the fox tapeworm *Echinococcus multilocularis* which causes a rare but fatal liver infection in humans. They showed that landscape metrics, derived from Landsat MSS and Landsat TM imagery were related to the prevalence of tapeworm infection for 31 villages in Zhang County, China. A summary of the use of discrete remote sensing imagery products in public health research are found in Table 2.

Table 2. Summary of literature in public health using discrete data products.*

Remotely Sensed Data	Remotely Sensed Variables/Target	Location	Application (Disease/Substance)	Reference
IKONOS	Land cover	Kenya	Vector-borne disease modeling (Malaria)	[88]
SPOT, IKONOS	Land cover	Belize	Vector-borne disease modeling (Malaria)	[87]
SPOT	Land cover	Belize	Vector-borne disease modeling (Malaria)	[93]
SPOT	Land cover	Burkina Faso	Vector-borne disease modeling (Malaria)	[95]
Aerial orthophoto, Landsat TM	Land cover, NDVI	California	Exposure modeling (Pesticide)	[22]
NLCD	Land cover	New England, USA	Exposure modeling (Arsenic)	[16]
Landsat TM	Land cover	Sichuan, China	Vector-borne disease modeling (Schistosomiasis)	[86]
Landsat TM & ETM+	Land cover	Central Wyoming	Vector-borne disease modeling (West Nile Virus)	[85]
Landsat ETM+	Land cover	Cape Cod, Massachusetts	Exposure modeling (Pesticide)	[89]
Landsat MSS & TM	Land cover	Western China	Vector-borne disease modeling (E. multilocularis)	[103-104]
Landsat MSS	Land cover	Iowa	Exposure modeling (Pesticide)	[90]
Landsat ETM+	Land cover	Paraguay	Vector habitat (Hantavirus)	[54]
ASTER	Land cover, LST	Cook County, Illinois	Vector-borne disease modeling (West Nile Virus)	[102]

*Note: ETM: Enhanced Thematic Mapper; TM: Thematic Mapper; MSS: Multispectral Scanner System; SPOT: Système Pour l'Observation de la Terre; ASTER: Advanced Spaceborne Thermal Emission and Reflection Radiometer; NDVI: Normalized Difference Vegetation Index; LST: Land Surface Temperature; NLCD: National Land Cover Database.

4. Object-Based Image Analysis

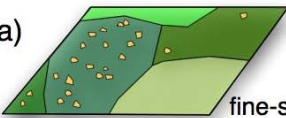
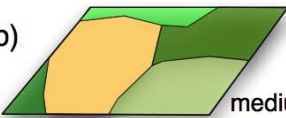
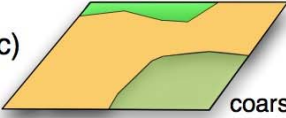
The land use/land cover mapping discussed in the previous section all resulted from image classification, either supervised or unsupervised, in a pixel-based paradigm. As discussed earlier, these pixel-based clustering algorithms focus only on the spectral value of each pixel and often result in image speckle and overall inaccuracies when applied to fine-resolution imagery [105]. This speckle, also known as the “salt-and-pepper” effect (Figure 1) is caused by high local spatial heterogeneity between neighboring pixels. Since each pixel is dealt with in isolation from its neighbors in the pixel-based paradigm, close neighbors often have different classes, despite being similar. When classification to produce discrete mapped entities is needed, an OBIA approach can alleviate many of these problems [30,33,37].

The OBIA approach includes two major steps: first the image is segmented into similar image objects (or segments) (Figure 2) and then the objects are classified based on attributes of and interrelations between segmented objects [106,107]. The basic processing units in OBIA are thus segments and not single pixels [31,106], and the process typically transforms a raster image into a vector format: most segments are operationally analyzed as polygons. The image segmentation concept is not new, and has been widely studied especially in the field of pattern recognition [30,31,108]. Recent developments in computational power have made older segmentation algorithms more useful in a mapping context. Once an object is created, meaningful spectral, spatial and contextual measures can be gathered about each object, and between adjacent objects in one dimension and across scale (Figure 3). These measures can be used to classify each object, at each scale. In Figure 3(a), the fine-scale objects (the small orange objects) segmented in the image are characterized by their spectral (e.g., spectral values for each object in each band, texture measures), spatial (e.g., their size, shape of each object), and contextual (e.g., their closest nearest neighbor, what is surrounding them) measures. These measures can be used to classify each fine-scale feature, which might be dead trees, or mosquito ponds, or other fine-scale discrete objects. At the medium-scale, these measures are also important, but they are calculated for the larger objects that include the fine-scale objects. In Figure 3(b), the orange polygon is a collection of smaller features, and in addition to the spectral, spatial, and contextual measures calculated for it, but it is the contextual information about its constituent finer-scale objects that can help in classification. For example, this medium-scale object might be a forest stand containing dead trees, or a marsh with surface ponds. The presence and patterning of the finer-scale objects might be useful in making this determination. The coarse-scale features are made of medium-scale features, and in a similar fashion, the medium-scale characteristics can be used to classify the coarse-scale object—as a forest, or a marsh complex. These multi-scalar classification concepts are modified from [31,33].

The relationships between an object and its neighbors across scales as shown in Figure 3 are not possible in pixel-based approaches. The topological relationships between adjacent pixels is implied in the raster data structure (meaning that the spatial relationship of each individual pixel does not need to be explicitly formulated), the topology and interaction of adjacent image objects is explicitly determined and each object explicitly described in the OBIA approach [106]. The resulting topological network is far more cumbersome to store, but it does allow for those relationships to be used for

subsequent analysis: either in object classification [31], or for higher order analysis of pattern and context in an ecological context.

Figure 3. Conceptual diagram of the OBIA process for multi-scaled analysis of remotely sensed imagery. (a), (b) and (c) are different levels of image segmentation (fine-scale to coarse-scale); they are hierarchical. At each scale the target is highlighted in orange. The characteristics are those spectral, spatial and contextual measures that can be used to classify an object. Only a few examples of characteristics within each category are listed, but there are many valuable measures at each scale that can be used for analysis depending on the research question (e.g., average, minimum, maximum, composite indexes, etc.). Fine-scale characteristics can be used to classify medium-scale features and so on.

Segmentation		Characteristics		
a)	 fine-scale	spectral - individual band information - texture - ...	spatial - size - shape - orientation - ...	contextual - nearest neighbors - surrounding objects -...
b)	 medium-scale	- spectral characteristics of fine-scaled objects -...	- presence of features at the fine-scale - pattern of features at the fine-scale -...	- contextual information from the fine-scaled objects - ...
c)	 coarse-scale	-spectral characteristics of medium-scaled objects -...	- presence of features at the medium-scaled objects - pattern of features at the medium-scaled objects -...	- contextual information from the medium-scaled objects -...

The improved classification that typically results from OBIA are often reported in the remote sensing literature across a range of applications [30]. As evidenced in the following paragraphs, many researchers are choosing OBIA approaches to map discrete landscape features because the method typically results in higher accuracies than classification with pixel-based approaches (e.g., [54,55,61,109]). We could find no examples of object-based approaches in public health that made use of the topological and hierarchical benefits conveyed by the OBIA approach.

5. Review of OBIA and Public Health Applications

Object based approaches to classification are most often used with fine-resolution (*i.e.*, <5 m) imagery (although not always), when pixel-based methods have proven problematic, and when discrete patches or features are the mapping target. Examples that pertain to public health can be found in the mapping of vector habitat, in land use/land cover mapping, and increasingly, in urban applications that examine urban structure as it influences health outcomes. What follows is a short review—OBIA approaches are only recently being integrated into public health research. These papers are summarized in Table 3.

Table 3. Summary of literature in public health using object-based image analysis.*

Remotely Sensed Data	Remotely Sensed Variables/Target	Location	Application (Disease/Condition)	Reference
Panchromatic aerial image	Panchromatic band/buildings	Golcuk, Turkey	Natural hazard damage assessment (Earthquake)	[110]
Lidar, QuickBird	Elevation, Land cover	Tegucigalpa, Honduras	Social vulnerability (Natural hazards)	[111]
QuickBird	Land cover	Kazakhstan	Vector habitat (Bubonic Plague)	[112]
QuickBird	Land cover	Accra, Ghana	Social vulnerability (Slum mapping)	[113]
QuickBird	NDVI, Land cover	Northern Darfur, Sudan	Humanitarian aid assessment (Population characteristics)	[114]
QuickBird	Land cover	Bam, Iran	Natural hazard damage assessment (Earthquake)	[115]
IKONOS	Land cover	Palestine & Republic of Macedonia	Natural hazard damage assessment (Earthquake)	[116]
IKONOS	Land cover	New York City, New York	Hazard mitigation (Urban heat island effect)	[109]
Aerial orthophoto, Landsat	Land cover, NDVI	California	Exposure modeling (Pesticide)	[22]
Landsat ETM+	Land cover	Paraguay	Vector habitat (Hantavirus)	[54]
MODIS, ASTER, QuickBird	EVI, NDVI, Land cover	Costa Rica	Vector-borne disease modeling (Dengue Fever)	[61]
ASTER	Land cover	China	Exposure modeling (Pollution)	[55]

*Note: OBIA: Object-based image analysis; ETM: Enhanced Thematic Mapper; Lidar: Light Detection and Ranging; ASTER: Advanced Spaceborne Thermal Emission and Reflection Radiometer; MODIS: Moderate Resolution Imaging Spectroradiometer; NDVI: Normalized Difference Vegetation Index; EVI: Enhanced Vegetation Index.

Addink *et al.* [112] provide a clear case study for the use of OBIA in mapping vector habitat. In Kazakhstan the great gerbil (*Rhombomys opimus*) hosts a flea that is the primary vector for the Bubonic plague bacteria *Yersinia pestis*. Their burrow systems are considered a strong indicator for the probability of a plague outbreak. They are also a good target for remote sensing, being large, more or less circular complex constructions with a diameter of 15 to 40 m displaying a lack of vegetation above and around them, due to herbivory by the gerbils. Their OBIA approach used QuickBird imagery, and resulted in very high classification accuracies: overall classification accuracy was 96%; where 98% of the observed burrow-systems were identified correctly, and 93% of the non-burrow-system segments were classified correctly. An OBIA approach also worked well for Koch *et al.* [54], who needed to classify land cover classes related to the movement and abundance of rodent species that are hosts to hantavirus. They used a single Landsat ETM+ image to classify land use/land cover into eight classes using both per-pixel and object-based classification algorithms at an Atlantic Forest site in eastern

Paraguay. Largely a proof-of-concept paper, they report on the far superior classification results provided by the OBIA approach.

As is clear from the previous paragraphs, much of the work examining the utility of remote sensing for vector-borne diseases have occurred in ex-urban settings, and the study of vector-borne diseases in urban environments is more difficult due to urban spatial heterogeneity and complexity, the complex movement of hosts and vectors, and anthropogenic creation of often fine-scale vector habitats [61]. Dengue fever is an example of a disease that affects urban dwellers. Its mosquito vector, *Aedes aegypti*, lives in close association with humans mostly in urban and suburban environments in fine-scale micro-habitats that are impossible to capture via remote sensing because they are too small or are hidden. Troyo *et al.* [61] used a combination of imagery and methods to study the spatial and seasonal determinants of dengue incidence in Costa Rica. In addition to examining dengue incidence and temporal NDVI dynamics, they also mapped urban land use/land cover classes and performed a landscape metric analysis to ascertain if urban land cover patterning could indicate dengue incidence. They compared both pixel-based and object-based classification approaches; the OBIA method proved more accurate. They found a moderate positive relationship between urban tree cover and dengue incidence and a significant relationship between the proportion of built area and dengue incidence. Furthermore, their landscape metric analysis showed that urban patterning (overall clumpiness index, percentage of like adjacencies for built areas, and patch cohesion for trees) showed strong significant correlations with dengue incidence.

Chemical or other exposure assessment applications require detailed land use/land cover maps before the spatial relationship of exposure sources and individuals or households can be assessed. An OBIA approach works well in this case. Maxwell [22] demonstrated an OBIA approach for delineating land use/land cover features at multiple scales using a fine spatial resolution aerial photograph (1 m) and a moderate spatial resolution Landsat image (30 m) time series in the context of examining exposure from pesticide spray drift. Her work largely aimed to prove the utility of such an approach, and she highlights one of the additional advantages of OBIA over pixel-based approaches to classification, other than overall accuracy: the spatial fidelity of the resulting objects. She concludes that maps derived from a pixel-based approach have to have an explicit topology in their output. Crop fields in a pixel-based product are collections of similarly-classified pixels, without spatial cohesion. This can have a substantial impact on epidemiological studies that do not consider spatial context. The OBIA approach facilitates a more complete representation and characterization of crop fields that classifies a field as an intact entity rather than a collection of pixels: this representation can support agricultural chemical exposure assessment [22].

An interesting case that used OBIA with moderate spatial resolution imagery is provided by Gao *et al.* [55] who mapped coal fires with ASTER imagery in China. These exposures are a threat to human health, and are a large problem in China [55]. The imagery was segmented using a multi-resolution segmentation algorithm in eCognition, and the resulting objects' spectral and spatial information (size, shape, texture and relations to other image objects) were used in classification.

There is also a small but growing body of OBIA work that focuses on other aspects of public health such as disaster recovery, urban crowding, and their related health consequences. Urban environments have proven fertile ground for OBIA researchers (e.g., [109]), as they are filled with discrete entities at multiple scales. Many of the following studies are reviewed in Blaschke [30].

Spatial variation in urban densities and amenities can influence poverty and health [117], and understanding such patterning can help target public health interventions. But spatial analysis of such urban patterns often has to deal with datasets of different reporting units and scales, and results based on combinations of such datasets are often flawed [118]. To overcome this challenge, Stow and colleagues [113] used OBIA with QuickBird imagery to correctly map urban densities and amenities at two scales in Accra, Ghana. They found their segmentation and hierarchical classification to be 75% accurate. Ebert and colleagues [111] take a different approach to arrive at an understanding of urban social vulnerability. They applied OBIA methods for the definition and estimation of variables from optical and Light Detection and Ranging (Lidar) data in combination with elevation information and existing hazard information. They sought to estimate a physical social vulnerability index that could be compared to census data available for the study area on a neighborhood level in Tegucigalpa, Honduras. The physical model of social vulnerability explained almost 60% of the variance found in the census data. They suggest that contextual segmentation-based analysis of geospatial data can substantially aid in urban assessment and public health screening because it provides a more economical and optimized workflow.

Lang *et al.* [114] applied OBIA methods on a series of QuickBird imagery of the Zam Zam internally displaced person (IDP) camp in Northern Darfur to follow the camp's evolution between 2002 and 2008. They mapped the camp's boundaries and inner structure, and derived population estimates for the time of image capture through a rule-based procedure. They assessed their ability to map individual dwellings (accuracies ranged from 71.6% to 94.9%) and estimated camp occupancy (with reference figures for dwelling occupancy obtained from estimates made by aid agencies).

Turker and Sumer [110] detected damaged buildings from an earthquake in Golcuk, Turkey, one of the urban areas most strongly affected by the 1999 Izmit earthquake. They used a creative shadow-based filter on fine spatial resolution imagery with a watershed segmentation algorithm to detect and map damaged or undamaged buildings. Gusella *et al.* [115] quantified the number of buildings that collapsed following the 2003 Bam earthquake, by first segmenting pre-earthquake Quickbird imagery and then comparing the spectral signature of those objects in the post-earthquake imagery. They report an overall accuracy of 70% for the damage classification. Change detection is a robust method for identifying these kinds of fine-scale changes. Al-Khudairy *et al.* [116] analyzed structural damage caused by conflicts using pre-conflict IKONOS images of Jenin (2 m resolution), in the Palestinian territories, and Brest (1 m resolution) in the former Yugoslav Republic of Macedonia. They showed that object-oriented segmentation and classification systems of pre- and post-conflict facilitated the interpretation of change detection results derived from fine-resolution (e.g., 1 m and 2 m) commercial satellite data.

We recognize that these examples are few in number, and we believe that there are many additional new directions in public health research and practice that can benefit from OBIA. For instance OBIA may be used to help in research that requires multi-scalar analysis, such as collecting census statistics in rural or developing areas. Through the use of OBIA, researchers could identify individual homes and other aspects of the built environment, including size, distribution and location, allowing for an enhanced understanding about where people live, and their distances to available facilities. OBIA could also be beneficial in public health research related to changes over time. In food security research, for example, it is essential to accurately account for the temporal variability of the size,

shape, and relative productivity of individual fields to estimate the nutritional output of croplands in areas at risk of famine. After the initial segmentation and classification of a complex array of diverse fields, it may be possible to more easily update the initial map in order to record change over time. Both of these multi-scalar and multi-temporal qualities are increasingly important in assessing the public health impacts of a changing climate.

6. Discussion and Conclusions

In this paper we have reviewed the large and diverse role of remote sensing in the public health field. We covered the use of continuous products such as NDVI in modeling risk and spread of vector-borne diseases around the world and obesity in urban environments. We covered the use of discrete mapping to capture vector habitat and other health exposures through land use/land cover mapping. We explore the relative lack of examples of OBIA approaches in this second category, and highlighted some important cases—in vector habitat and exposure mapping, and in new areas of indirect public health outcomes where the OBIA approach has a natural fit. We also describe possibilities for additional uses of OBIA in public health.

Most of the examples presented here highlight the accuracy benefits of the OBIA approach over that of the pixel-based approach, but we contend that there are key areas when the depiction of a geographic object as an image object in an OBIA sense—as a multi-scale object, that carries knowledge, that has shape—is useful. In ecology, for example, there are situations where the object framework is integral to the understanding of the function of an ecological system. While in many ecological systems species success and productivity respond to ecological gradients and produce transitional patterns across spatial scales (e.g., [119]), in other systems, due to disturbance, thresholds in ecological response, or management, vegetation pattern will be naturally discrete. In these cases, ecological objects appear with defined edges, such as treeline [38], or gaps in forests [34], or seagrass beds [120]. In a landscape ecological sense [121], these “objects” are also characterized by the topological relationships with their neighbors, in space and time. Proximity, context and pattern through time can influence functional processes of succession, survival and spread (e.g., [9,122]). In addition, these ecological objects display hierarchies, and can be characterized by connections across multiple scales. And while these kinds of multi-scaled patterns can be used to construct rules for classifying image objects and refining classification results in an OBIA framework (e.g., [31,55]), they can also convey important agency to the resulting objects, in certain contexts, and give us added ecological and epidemiological insight to many systems. For example, Wallentin [38] found an OBIA approach’s ability to measure pattern fundamental to understanding the function of treeline dynamics in the Austrian Central Alps. In a public health setting, these topological features can be just as useful. For example, with vector habitat mapping, knowing that mosquito ponds are more densely arrayed in certain types of land use could be an added component to predicting risk for malaria. Knowing that snail habitats are more or less connected to village land uses could help understand schistosomiasis spread. Knowing how the crop type in one field changes, and how its neighbors also change can help pesticide exposure studies.

It is important to concede that these kinds of relationships can be built after-the-fact within a geographic information system (GIS) from any classification result [102-104], but they are more easily

done as part of the classification process with OBIA. Indeed, such landscape analyses of pixel-based products are flawed, due to the speckle inherent in the results. Such products require considerable post processing to deal with these artifacts, processing that can change the inherent spatial relationships one wants to preserve [35]. The OBIA approach keeps relevant objects intact (this was the point Maxwell [22] raised about crop fields) and can elucidate relationships between objects and sub-objects. Figure 3 demonstrates this conceptually. In an ecological sense the finer-scale objects can be dead trees in a forest stand using information about the presence and distribution of these trees, forest stands can be classified as to their degree of disease infestation [123,124]. Alternatively, in an epidemiological sense, these features might be mosquito ponds in a larger marsh or wet soil area; their abundance and distribution might help characterize risk for a neighboring village. It is this kind of contextual information about objects that proved so useful for Liu and Weng [102] and Graham and colleagues [103,104] in their examination of pattern and disease.

Burnett and Blaschke [33] state that there are multiple solutions to the decomposition of a landscape: some utilize a continuous or field-based model, and some a discrete-based model. While there are theoretical developments to unite these two representations (e.g., [125]), often the choice of format has to do with purpose, subsequent analysis, and convention. Sometimes one format is superior to another in one context. Cohen and colleagues [126] found that land use/land cover mapping did not help in predicting household malaria risk in western Kenya. They used an OBIA approach with IKONOS imagery to map land use/land cover surrounding households for which they had demographic data and information on malaria events. In their case the continuous data format was more useful. Variables related to topographic wetness proved most useful in predicting the households of individuals contracting malaria in the region, suggesting that the rugged terrain in the study area imparted a larger influence on vector habitat through accumulation of water than did land use/land cover. Yet whenever a discrete set of interrelated spatial features is needed to understand the functioning of a system, be it an ecological or an epidemiological one, an OBIA approach offers many advantages in accuracy, and in analysis.

Given the dynamic nature of our landscape and increasing rate of change due to rising populations and changing climates, OBIA can provide a platform to quickly and effectively monitor these changes over large areas. Many of the existing studies that have used OBIA to better understand public health challenges, such as disease vectors, heat island effects, and toxin exposure have shown the value that these techniques can provide. We encourage even further exploration of these same methods to scale up their benefits to additional areas in need of greater research and monitoring. As the cost and technological barriers to using OBIA and fine resolution imagery continue to decline, we hope to see greater use of these tools. Good places to start using OBIA for image classification and analysis are: Blaschke [30], Benz and colleagues [106], Maxwell [22], and Navulur [127]. There are also a large and increasing range of software packages that perform image segmentation and object-based classification analyses, including as mentioned before eCognition [52,53], but also ENVI's Feature Extraction Module [128], Visual Learning Systems' Feature Analyst extension for ArcGIS [129], ERDAS IMAGINE's Objective module [130] and IDRISI Taiga's Segmentation module [131] to name a few.

References

1. Cohen, W.B.; Goward, S.N. Landsat's role in ecological applications of remote sensing. *BioScience* **2004**, *54*, 535-545.
2. Wulder, M.A.; Hall, R.J.; Coops, N.C.; Franklin, S.E. High spatial resolution remotely sensed data for ecosystem characterization. *BioScience* **2004**, *54*, 511-521.
3. Wulder, M.A.; Dymond, C.C.; White, J.C.; Leckie, D.G.; Carroll, A.L. Surveying mountain pine beetle damage of forests: A review of remote sensing opportunities. *Forest Ecol. Manage.* **2006**, *221*, 27-41.
4. Chambers, J.Q.; Fisher, J.I.; Zeng, H.; Chapman, E.L.; Baker, D.B.; Hurtt, G.C. Hurricane Katrina's carbon footprint on US gulf coast forests. *Science* **2007**, *318*, 1107.
5. DeFries, R.; Achard, F.; Brown, S.; Herold, M.; Murdiyarto, D.; Schlamadinger, B.; de Souza, C., Jr. Earth observations for estimating greenhouse gas emissions from deforestation in developing countries. *Environ. Sci. Policy* **2007**, *10*, 385-394.
6. Foley, J.A.; DeFries, R.; Asner, G.P.; Barford, C.; Bonan, G.; Carpenter, S.R.; Chapin, F.S.; Coe, M.T.; Daily, G.C.; Gibbs, H.K.; *et al.* Global consequences of land use. *Science* **2005**, *309*, 570-574.
7. Homer, C.; Dewitz, J.; Fry, J.; Coan, M.; Hossain, N.; Larson, C.; Herold, N.; McKerrow, A.; VanDriel, J.N.; Wickham, J. Completion of the 2001 National Land Cover Database for the monoterminous United States. *Photogramm. Eng. Remote Sensing* **2007**, *73*, 337-341.
8. DeFries, R.S.; Townshend, J.R.G. Global land cover characterization from satellite data: From research to operational implementation. *Global Ecol. Biogeogr.* **1999**, *8*, 367-379.
9. Pringle, R.M.; Doak, D.F.; Brody, A.K.; Jocque, R.; Palmer, T.M. Spatial pattern enhances ecosystem functioning in an african savanna. *PLoS Biol.* **2010**, *8*, 1-12.
10. Smith, B.; Knorr, W.; Widlowski, J.L.; Pinty, B.; Gobron, N. Combining remote sensing data with process modelling to monitor boreal conifer forest carbon balances. *Forest Ecol. Manage.* **2008**, *255*, 3985-3994.
11. Running, S.W.; Baldocchi, D.D.; Turner, D.P.; Gower, S.T.; Bakwin, P.S.; Hibbard, K.A. A Global Terrestrial Monitoring Network integrating tower fluxes, flask sampling, ecosystem modeling and EOS satellite data. *Remote Sens. Environ.* **1999**, *70*, 108-127.
12. Bartlett, D.S.; Klemas, V. Quantitative assessment of tidal wetlands using remote sensing. *Environ. Manage.* **1980**, *4*, 337-345.
13. Anderson, J.R. Land use classification schemes used in selected geographic applications in remote sensing. *Photogramm. Eng. Remote Sensing* **1971**, *37*, 379-387.
14. Herbreteau, V.; Salem, G.; Souris, M.; Hugot, J.P.; Gonzalez, J.P. Thirty years of use and improvement of remote sensing, applied to epidemiology: From early promises to lasting frustration. *Health Place* **2007**, *13*, 400-403.
15. Kalluri, S.; Gilruth, P.; Rogers, D.; Szczur, M. Surveillance of arthropod vector-borne infectious diseases using remote sensing techniques: A review. *PLoS Pathog.* **2007**, *3*, e116.
16. Ayotte, J.D.; Nolan, B.T.; Nuckols, J.R.; Cantor, K.P.; Robinson, G.R., Jr.; Baris, D.; Hayes, L.; Karagas, M.; Bress, W.; Silverman, D.T. Modeling the probability of arsenic in groundwater in New England as a tool for exposure assessment. *Environ. Sci. Technol.* **2006**, *40*, 3578-3585.

17. Krause, G.; Bock, M.; Weiers, S.; Braun, G. Mapping land-cover and mangrove structures with remote sensing techniques: A contribution to a synoptic GIS in support of coastal management in North Brazil. *Environ. Manage.* **2004**, *34*, 429-440.
18. Beck, L.R.; Lobitz, B.M.; Wood, B.L. Remote sensing and human health: New sensors and new opportunities. *Emerg. Infect. Dis.* **2000**, *6*, 217.
19. Simoonga, C.; Utzinger, J.; Brooker, S.; Vounatsou, P.; Appleton, C.; Stensgaard, A.S.; Olsen, A.; Kristensen, T.K. Remote sensing, geographical information system and spatial analysis for schistosomiasis epidemiology and ecology in africa. *Parasitology* **2009**, *136*, 1683-1693.
20. Zhou, X.; Malone, J.; Kristensen, T.; Bergquist, N., Application of geographic information systems and remote sensing to schistosomiasis control in China. *Acta Trop.* **2001**, *79*, 97-106.
21. Brooker, S.; Hay, S.; Tchuem, L.; Ratard, R. Using NOAA-AVHRR data to model human health distribution on planning disease control in Cameroon, West Africa. *Photogramm. Eng. Remote Sensing* **2002**, *68*, 175-179.
22. Maxwell, S.K. Generating land cover boundaries from remotely sensed data using object-based image analysis: Overview and epidemiological application. *Spatial Spatio-Temporal Epidemiol.* **2010**, *1*, 231-237.
23. Griffith, J.A.; Marinko, E.A.; Whistler, J.L.; Price, K.P. Interrelationships among landscapes, NDVI, and stream water quality in the U.S. central plains. *Ecol. Appl.* **2002**, *12*, 1702-1718.
24. Ji, L.; Peters, A.J. Lag and seasonality considerations in evaluating AVHRR NDVI response to precipitation. *Photogramm. Eng. Remote Sensing* **2005**, *71*, 1053-1061.
25. Hansen, M.; DeFries, R.; Townshend, J.; Sohlberg, R.; Dimiceli, C.; Carroll, M. Towards an operational MODIS continuous field of percent tree cover algorithm: Examples using AVHRR and MODIS data. *Remote Sens. Environ.* **2002**, *83*, 303-319.
26. Xian, G.; Homer, C. Updating the 2001 National Land Cover database impervious surface products to 2006 using Landsat Imagery Change Detection Methods. *Remote Sens. Environ.* **2010**, *114*, 1676-1686.
27. Chabaeva, A.; Civco, D.L.; Hurd, J.D. Assessment of impervious surface estimation techniques. *J. Hydrol. Eng.* **2009**, *14*, 377.
28. He, H.; Mladenoff, D.; Boeder, J. An object-oriented forest landscape model and its representation of tree species. *Ecol. Model.* **1999**, *119*, 1-19.
29. Cohen, J.M.; Ernst, K.C.; Lindblade, K.A.; Vulule, J.M.; John, C.C.; Wilson, M.L. Topography-derived wetness indices are associated with household-level malaria risk in two communities in the western Kenyan highlands. *Malaria J.* **2008**, *7*, 40.
30. Blaschke, T. Object based image analysis for remote sensing. *ISPRS J. Photogramm.* **2010**, *65*, 2-16.
31. Liu, Y.; Guo, Q.; Kelly, M. A framework of region-based spatial relationships for non-overlapping features and its application in object based image analysis. *ISPRS J. Photogramm.* **2008**, *63*, 461-475.
32. Townshend, J.R.G.; Huang, C.; Kalluri, S.N.V.; DeFries, R.S.; Liang, S. Beware of per-pixel characterization of land cover. *Int. J. Remote Sens.* **2000**, *21*, 839-843.
33. Burnett, C.; Blaschke, T. A multi-scale segmentation/object relationship modelling methodology for landscape analysis. *Ecol. Model.* **2003**, *168*, 233-249.

34. DeChant, T.; Kelly, M. Individual object change detection for monitoring the impact of a forest pathogen on a hardwood forest. *Photogramm. Eng. Remote Sensing* **2009**, *75*, 1005-1014.
35. Kelly, M.; Tuxen, K.; Stralberg, D. Mapping changes to vegetation pattern in a restoring wetland: Finding pattern metrics that are consistent across scale and time. *Ecol. Indic.* **2011**, *11*, 263-273.
36. Rocchini, D.; Perry, G.; Salerno, M.; Maccherini, S.; Chiarucci, A. Landscape change and the dynamics of open formations in a natural reserve. *Landscape Urban Plan.* **2006**, *77*, 167-177.
37. Langanke, T.; Burnett, C.; Lang, S. Assessing the mire conservation status of a raised bog site in Salzburg using object-based monitoring and structural analysis. *Landscape Urban Plan.* **2007**, *79*, 160-169.
38. Wallentin, G.; Tappeiner, U.; Strobl, J.; Tasser, E. Understanding alpine tree line dynamics: An individual-based model. *Ecol. Model.* **2008**, *218*, 235-246.
39. Guo, Q.C.; Kelly, M.; Gong, P.; Liu, D. An object-based classification approach in mapping tree mortality using high spatial resolution imagery. *GISci. Remote Sens.* **2007**, *44*, 24-47.
40. Liu, D.; Kelly, M.; Gong, P.; Guo, Q. Characterizing spatial-temporal tree mortality patterns associated with a new forest disease. *Forest Ecol. Manage.* **2007**, *253*, 220-231.
41. Cleve, C.; Kelly, M.; Kearns, F.; Moritz, M. Classification of urban environments for fire management support: A comparison of pixel- and object-based classifications using high-resolution aerial photography. *Comput. Environ. Urban Syst.* **2008**, *32*, 317-326.
42. Walsh, S.J.; McCleary, A.L.; Mena, C.F.; Shao, Y.; Tuttle, J.P.; González, A.; Atkinson, R. QuickBird and Hyperion data analysis of an invasive plant species in the Galapagos Islands of Ecuador: Implications for control and land use management. *Remote Sens. Environ.* **2008**, *112*, 1927-1941.
43. Tosun, A.B.; Kandemir, M.; Sokmensuer, C.; Gunduz-Demir, C. Object-oriented texture analysis for the unsupervised segmentation of biopsy images for cancer detection. *Pattern Recogn.* **2009**, *42*, 1104-1112.
44. Krecsák, L.; Micsik, T.; Kiszler, G.; Krenács, T.; Szabo, D.; Jonás, V.; Császár, G.; Czuni, L.; Gurzo, P.; Ficsor, L.; Molnar, B. Technical note on the validation of a semi-automated image analysis software application for estrogen and progesterone receptor detection in breast cancer. *Diagn. Pathol.* **2011**, *6*, 6.
45. Lamprecht, M.R.; Sabatini, D.M.; Carpenter, A.E. CellProfiler: Free, versatile software for automated biological image analysis. *Biotechniques* **2007**, *42*, 71.
46. Zimmer, C.; Labruyere, E.; Meas-Yedid, V.; Guillen, N.; Olivo-Marin, J.C. Segmentation and tracking of migrating cells in videomicroscopy with parametric active contours: A tool for cell-based drug testing. *IEEE Trans. Med. Imag.* **2002**, *21*, 1212-1221.
47. Lehmann, T.M.; Gold, M.; Thies, C.; Fischer, B.; Spitzer, K.; Keysers, D.; Ney, H.; Kohlen, M.; Schubert, H.; Wein, B.B. Content-based image retrieval in medical applications. *Method. Inform. Med.* **2004**, *43*, 354-361.
48. Megason, S.G.; Fraser, S.E. Digitizing life at the level of the cell: High-performance laser-scanning microscopy and image analysis for in toto imaging of development. *Mech. Develop.* **2003**, *120*, 1407-1420.

49. Carpenter, A.E.; Jones, T.R.; Lamprecht, M.R.; Clarke, C.; Kang, I.H.; Friman, O.; Guertin, D.A.; Chang, J.H.; Lindquist, R.A.; Moffat, J. CellProfiler: Image analysis software for identifying and quantifying cell phenotypes. *Genome Biol.* **2006**, *7*, R100.
50. Yu, Q.; Gong, P.; Clinton, N.; Kelly, M.; Shirokauer, D. Object-based detailed vegetation classification with airborne high resolution remote sensing imagery. *Photogramm. Eng. Remote Sensing* **2006**, *72*, 799-811.
51. Hashim, M.; Mohd Noor, N.; Marghany, M. Modeling sprawl of unauthorized development using geospatial technology: Case study in Kuantan District, Malaysia. *Int. J. Digital Earth* **2010**, *4*, 223-238.
52. Trimble. eCognition. *Trimble GeoSpatial*. Available online: <http://www.trimble.com/geospatial/> (accessed on 20 October 2011).
53. Trimble. *eCognition Developer 8.64.0: User Guide*; Trimble: Munich, Germany, 2010.
54. Koch, D.E.; Mohler, R.L.; Goodin, D.G. Stratifying land use/land cover for spatial analysis of disease ecology and risk: An example using object-based classification techniques. *Geospatial Health* **2007**, *2*, 15-28.
55. Gao, Y.; Kerle, N.; Mas, J.F. Object-based image analysis for coal fire-related land cover mapping in coal mining areas. *GeoCarto Int.* **2009**, *24*, 25-36.
56. Lo, C.; Faber, B.J. Integration of landsat thematic mapper and census data for quality of life assessment. *Remote Sens. Environ.* **1997**, *62*, 143-157.
57. Hatfield, J. Remote sensing estimators of potential and actual crop yield. *Remote Sens. Environ.* **1983**, *13*, 301-311.
58. Quarmby, N.; Milnes, M.; Hindle, T.; Silleos, N. The use of multi-temporal NDVI measurements from avhrr data for crop yield estimation and prediction. *Int. J. Remote Sens.* **1993**, *14*, 199-210.
59. Townsend, F.E. The enhancement of computer classifications by logical smoothing. *Photogramm. Eng. Remote Sensing* **1986**, *52*, 213-221.
60. Green, R.M.; Hay, S.I. The potential of pathfinder avhrr data for providing surrogate climatic variables across africa and europe for epidemiological applications. *Remote Sens. Environ.* **2002**, *79*, 166-175.
61. Troyo, A.; Fuller, D.O.; Calderon Arguedas, O.; Solano, M.E.; Beier, J.C. Urban structure and dengue incidence in puntarenas, costa rica. *Singapore J. Trop. Geo* **2009**, *30*, 265-282.
62. Estrada-Peña, A. Increasing habitat suitability in the united states for the tick that transmits Lyme disease: A remote sensing approach. *Environ. Health Persp.* **2002**, *110*, 635.
63. Rogers, D.; Myers, M.; Tucker, C.; Smith, P.; White, D.; Backenson, P.; Eidson, M.; Kramer, L.; Bakker, B.; Hay, S. Predicting the distribution of west nile fever in north america using satellite sensor data. *Photogramm. Eng. Remote Sensing* **2002**, *68*, 112-136.
64. Linthicum, K.J.; Anyamba, A.; Tucker, C.J.; Kelley, P.W.; Myers, M.F.; Peters, C.J. Climate and satellite indicators to forecast Rift Valley fever epidemics in Kenya. *Science* **1999**, *285*, 397.
65. Bell, J.F.; Wilson, J.S.; Liu, G.C. Neighborhood greenness and 2-year changes in body mass index of children and youth. *Am. J. Prev. Med.* **2008**, *35*, 547-553.
66. Tilt, J.H.; Unfried, T.M.; Roca, B. Using objective and subjective measures of neighborhood greenness and accessible destinations for understanding walking trips and BMI in Seattle, Washington. *Health Promot.* **2007**, *21*, 371-379.

67. Jerrett, M.; McConnell, R.; Chang, C.C.R.; Wolch, J.; Reynolds, K.; Lurmann, F.; Gilliland, F.; Berhane, K. Automobile traffic around the home and attained body mass index: A longitudinal cohort study of children aged 10–18 years. *Prev. Med.* **2010**, *50*, Suppl 1, S50-8.
68. Wolch, J.; Jerrett, M.; Reynolds, K.; McConnell, R.; Chang, R.; Dahmann, N.; Brady, K.; Gilliland, F.; Su, J.G.; Berhane, K. Childhood obesity and proximity to urban parks and recreational resources: A longitudinal cohort study. *Health Place* **2010**, *17*, 207-214.
69. Dister, S.W.; Fish, D.; Bros, S.M.; Frank, D.H.; Wood, B.L. Landscape characterization of peridomestic risk for Lyme disease using satellite imagery. *Am. J. Trop. Med. Hyg.* **1997**, *57*, 687.
70. Liu, G.C.; Wilson, J.S.; Qi, R.; Ying, J. Green neighborhoods, food retail and childhood overweight: Differences by population density. *Am. J. Health Promot.* **2007**, *21*, 317-325.
71. Tucker, C.J.; Wilson, J.M.; Mahoney, R.; Anyamba, A.; Linthicum, K.; Myers, M.F. Climatic and ecological context of the 1994–1996 Ebola outbreaks. *Photogramm. Eng. Remote Sensing* **2002**, *68*, 147-152.
72. Johnson, D.P.; Wilson, J.S.; Luber, G.C. Socioeconomic indicators of heat-related health risk supplemented with remotely sensed data. *Int. J. Health Geogr.* **2009**, *8*, 57.
73. Stensgaard, A.; Jorgensen, A.; Kabatereine, N.; Malone, J.; Kristensen, T. Modeling the distribution of *Schistosoma mansoni* and host snails in Uganda using satellite sensor data and Geographical Information Systems. *Parassitologia* **2005**, *47*, 115-125.
74. Rogers, D.J.; Hay, S.I.; Packer, M.J. Predicting the distribution of tsetse-flies in West-Africa using temporal Fourier processed meteorological satellite data. *Ann. Trop. Med. Parasitol* **1996**, *90*, 225-241.
75. Hay, S.; Snow, R.; Rogers, D. From predicting mosquito habitat to malaria seasons using remotely sensed data: Practice, problems and perspectives. *Parasitol. Today* **1998**, *14*, 306-313.
76. Omumbo, J.; Hay, S.; Goetz, S.; Snow, R.; Rogers, D. Updating historical maps of malaria transmission duration in East Africa using remote sensing. *Photogramm. Eng. Remote Sensing* **2002**, *68*, 161-166.
77. Brooker, S.; Hay, S.I.; Issae, W.; Hall, A.; Kihamia, C.M.; Lwambo, N.J.S.; Wint, W.; Rogers, D.J.; Bundy, D.A.P. Predicting the distribution of urinary schistosomiasis in Tanzania using satellite sensor data. *Trop. Med. Int. Health* **2001**, *6*, 998-1007.
78. Anyamba, A.; Linthicum, K.; Mahoney, R.; Tucker, C.; Kellye, P. Mapping potential risk of rift valley fever outbreaks in African Savannas using vegetation index time series data. *Photogramm. Eng. Remote Sensing* **2002**, *68*, 137-146.
79. Hay, S.; Omumbo, J.; Craig, M.; Snow, R. Earth observation, geographic information systems and *Plasmodium falciparum* malaria in sub-Saharan Africa. *Adv. Parasitol.* **2000**, *47*, 173-174, IN175-IN112, 175-215.
80. Kauth, R.J.; Thomas, G. The Tasselled Cap—A Graphic Description of the Spectral-Temporal Development of Agricultural Crops as Seen by Landsat. In *Proceedings of the Symposium on Machine Processing of Remotely Sensed Data*, West Lafayette, IN, USA, 29 June–1 July 1976; pp. 41-51.
81. Cline, B.L. New eyes for epidemiologists: Aerial photography and other remote sensing techniques. *Am. J. Epidemiol.* **1970**, *92*, 85-89.

82. Hugh-Jones, M. Applications of remote sensing to the identification of the habitats of parasites and disease vectors. *Parasitol. Today* **1989**, *5*, 244-251.
83. Rogers, D.J.; Randolph, S.E.; Snow, R.W.; Hay, S.I. Satellite imagery in the study and forecast of malaria. *Nature* **2002**, *415*, 710-715.
84. Yang, G.J.; Vounatsou, P.; Xiao-Nong, Z.; Utzinger, J.; Tanner, M. A review of geographic information system and remote sensing with applications to the epidemiology and control of schistosomiasis in China. *Acta Trop.* **2005**, *96*, 117-129.
85. Zou, L.; Miller, S.N.; Schmidtman, E.T. Mosquito larval habitat mapping using remote sensing and GIS: Implications of coalbed methane development and West Nile virus. *J. Med. Entomol.* **2006**, *43*, 1034-1041.
86. Seto, E.; Xu, B.; Liang, S.; Gong, P.; Pu, W.; Davis, G.; Qui, D.; Gu, X.; Spear, R. The use of remote sensing for predictive modeling of schistosomiasis in China. *Photogramm. Eng. Remote Sensing* **2002**, *68*, 167-174.
87. Achee, N.L.; Grieco, J.P.; Masuoka, P.; Andre, R.G.; Roberts, D.R.; Thomas, J.; Briceno, I.; King, R.; Rejmankova, E. Use of remote sensing and geographic information systems to predict locations of *Anopheles darlingi*-positive breeding sites within the Sibun River in Belize, Central America. *J. Med. Entomol.* **2006**, *43*, 382-392.
88. Mutuku, F.; Bayoh, M.; Hightower, A.; Vulule, J.; Gimnig, J.; Mueke, J.; Amimo, F.; Walker, E. A supervised land cover classification of a western Kenya lowland endemic for human malaria: Associations of land cover with larval *Anopheles* habitats. *Int. J. Health Geogr.* **2009**, *8*, 19.
89. Brody, J.G.; Vorhees, D.J.; Melly, S.J.; Swedis, S.R.; Drivas, P.J.; Rudel, R.A. Using GIS and historical records to reconstruct residential exposure to large-scale pesticide application. *J. Expo. Anal. Env. Epid.* **2002**, *12*, 64-80.
90. Ward, M.H.; Lubin, J.; Giglierano, J.; Colt, J.S.; Wolter, C.; Bekiroglu, N.; Camann, D.; Hartge, P.; Nuckols, J.R. Proximity to crops and residential exposure to agricultural herbicides in Iowa. *Environ. Health Persp.* **2006**, *114*, 893.
91. Maxwell, S.K.; Meliker, J.R.; Goovaerts, P. Use of land surface remotely sensed satellite and airborne data for environmental exposure assessment in cancer research. *J. Expo. Anal. Env. Epid.* **2010**, *20*, 176-185.
92. Opperman, J.J.; Lohse, K.A.; Brooks, C.; Kelly, N.M.; Merenlender, A.M. Influence of land use on fine sediment in salmonid spawning gravels within the Russian River Basin, California. *Can. J. Fish. Aquat. Sci.* **2005**, *62*, 2740-2751.
93. Roberts, D.R.; Paris, J.F.; Manguin, S.; Harbach, R.E.; Woodruff, R.; Rejmankova, E.; Polanco, J.; Wullschleger, B.; Legters, L.J. Predictions of malaria vector distribution in Belize based on multispectral satellite data. *Am. J. Trop. Med. Hyg.* **1996**, *54*, 304.
94. Vogelmann, J.E.; Howard, S.M.; Yang, Y.; Larson, C.R.; Wylie, B.K.; Van Driel, N. Completion of the 1990s National Land Cover Data Set for the conterminous United States from Landsat Thematic Mapper Data and ancillary datasources. *Photogramm. Eng. Remote Sensing* **2001**, *67*, 650-652.
95. Dambach, P.; Sie, A.; Lacaux, J.-P.; Vignolles, C.C.; Machault, V.; Sauerborn, R. Using high spatial resolution remote sensing for risk mapping of malaria occurrence in the Nouna district, Burkina Faso. *Global Health* **2009**, doi:10.3402/gha.v2i0.2094.

96. Bedford, B.L. The need to define hydrologic equivalence at the landscape scale for freshwater wetland mitigation. *Ecol. Appl.* **1996**, *6*, 57-68.
97. Turner, M.G.; Gardner, R.H.; O'Neill, R.V. *Landscape Ecology in Theory and Practice: Pattern and Process*; Springer-Verlag: New York, NY, USA, 2001; p. 401.
98. Ostfeld, R.S.; Glass, G.E.; Keesing, F. Spatial epidemiology: An emerging (or re-emerging) discipline. *Trends Ecol. Evol.* **2005**, *20*, 328-336.
99. Uuemaa, E.; Antrop, M.; Roosaare, J.; Marja, R.; Mander, Ü. Landscape metrics and indices: An overview of their use in landscape research. *Liv. Rev. Landscape Res.* **2009**, *3*, 1.
100. McGarigal, K.; Marks, B. *FRAGSTATS: Spatial Pattern Analysis Program for Quantifying Landscape Structure*; Forest Science Department, Oregon State University: Corvallis, OR, USA, 1994; p. 62.
101. Kearns, F.R.; Kelly, N.M.; Carter, J.L.; Resh, V.H. A method for the use of landscape metrics in freshwater research and management. *Landscape Ecol.* **2005**, *20*, 113-125.
102. Liu, H.; Weng, Q. An examination of the effect of landscape pattern, land surface temperature, and socioeconomic conditions on WNV dissemination in Chicago. *Environ. Monit. Assess.* **2009**, *159*, 143-161.
103. Graham, A.; Danson, F.; Craig, P. Ecological epidemiology: The role of landscape structure in the transmission risk of the fox tapeworm *Echinococcus multilocularis* (Leukart 1863) (Cestoda: Cyclophyllidae: Taeniidae). *Prog. Phys. Geog.* **2005**, *29*, 77.
104. Graham, A.; Danson, F.; Giraudoux, P.; Craig, P. Ecological epidemiology: Landscape metrics and human alveolar echinococcosis. *Acta Trop.* **2004**, *91*, 267-278.
105. Kelly, M.; Shaari, D.; Guo, Q.H.; Liu, D.S. A comparison of standard and hybrid classifier methods for mapping hardwood mortality in areas affected by "sudden oak death". *Photogramm. Eng. Remote Sensing* **2004**, *70*, 1229-1239.
106. Benz, U.C.; Hofmann, P.; Willhauck, G.; Lingenfelder, I.; Heynen, M. Multi-resolution, object-oriented fuzzy analysis of remote sensing data for GIS-ready information. *ISPRS J. Photogramm.* **2004**, *58*, 239-258.
107. Blaschke, T.; Hay, G.J. Object-oriented image analysis and scale-space: Theory and methods for modeling and evaluating multiscale landscape structure. In *Proceedings of ISPRS WG IV/3, IV/5, IV/6 and IV/7 Workshop "Challenges in Geo-Spatial Analysis, Integration and Visualization"*, Athens, GA, USA, 29–31 October 2011; In *IAPRS*; 2001, Volume 34, Part 4/W5, pp. 22-29.
108. Pal, N.R.; Pal, S.K. A review on image segmentation techniques. *Pattern Recogn.* **1993**, *26*, 1277-1294.
109. Bhaskaran, S.; Paramananda, S.; Ramnarayan, M. Per-pixel and object-oriented classification methods for mapping urban features using Ikonos satellite data. *Appl. Geogr.* **2010**, *30*, 650-665.
110. Turker, M.; Sumer, E. Building-based damage detection due to earthquake using the watershed segmentation of the post-event aerial images. *Int. J. Remote Sens.* **2008**, *29*, 3073-3089.
111. Ebert, A.; Kerle, N.; Stein, A. Urban social vulnerability assessment with physical proxies and spatial metrics derived from air-and spaceborne imagery and GIS data. *Natural Hazards* **2009**, *48*, 275-294.

112. Addink, E.A.; de Jong, S.M.; Davis, S.A.; Dubyanskiy, V.; Leirs, H. Using Very High Spatial Resolution Remote Sensing to Monitor and Combat Outbreaks of Bubonic Plague in Kazakhstan. In *Proceedings of Anais XIV Simpósio Brasileiro de Sensoriamento Remoto*, Natal, Brazil, 25–30 April 2009; pp. 7529-7536.
113. Stow, D.; Lopez, A.; Lippitt, C.; Hinton, S.; Weeks, J. Object-based classification of residential land use within Accra, Ghana based on Quickbird satellite data. *Int. J. Remote Sens.* **2007**, *28*, 5167.
114. Lang, S.; Tiede, D.; Holbling, D.; Fureder, P.; Zeil, P. Earth observation (EO)-based ex post assessment of internally displaced person (IDP) camp evolution and population dynamics in Zam Zam, Darfur. *Int. J. Remote Sens.* **2010**, *31*, 5709-5731.
115. Gusella, L.; Adams, B.J.; Bitelli, G.; Huyck, C.K.; Mognol, A. Object-oriented image understanding and post-earthquake damage assessment for the 2003 Bam, Iran, earthquake. *Earthq. Spectra* **2005**, *21*, S225.
116. Al-Khudhairy, D.H.A.; Caravaggi, I.; Giada, S. Structural damage assessments from IKONOS data using change detection, object-oriented segmentation, and classification techniques. *Photogramm. Eng. Remote Sensing* **2005**, *71*, 825-837.
117. Weeks, J.R.; Hill, A.; Stow, D.; Getis, A.; Fugate, D. Can we spot a neighborhood from the air? Defining neighborhood structure in Accra, Ghana. *GeoJournal* **2007**, *69*, 9-22.
118. Spielman, S.E.; Yoo, E. The spatial dimensions of neighborhood effects. *Soc. Sci. Med.* **2009**, *68*, 1098-1105.
119. Watson, E.; Byrne, R. Abundance and diversity of tidal marsh plants along the salinity gradient of the San Francisco Estuary: Implications for global change ecology. *Plant Ecol.* **2009**, *205*, 113-128.
120. Kelly, N.M.; Fonseca, M.; Whitfield, P. Predictive mapping for management and conservation of seagrass beds in North Carolina. *Aquat. Conserv.* **2001**, *11*, 437-451.
121. Turner, M. Landscape ecology: The effect of pattern on process. *Ann. Rev. Ecol. Syst.* **1989**, *20*, 171-197.
122. Sousa, W.P. Intertidal mosaics: Patch size, propagule availability, and spatially variable patterns of succession. *Ecology* **1984**, *65*, 1918-1935.
123. Hay, G.; Castilla, G.; Wulder, M.A.; Ruiz, J.R. An automated object-based approach for the multiscale image segmentation of forest scenes. *Int. J. Appl. Earth Obs. Geoinf.* **2005**, *7*, 339-359.
124. Hay, G.J.; Blaschke, T.; Marceau, D.J.; Bouchard, A. A comparison of three image-object methods for the multiscale analysis of landscape structure. *ISPRS J. Photogramm.* **2003**, *57*, 327-345.
125. Goodchild, M.F.; Yuan, M.; Cova, T.J. Towards a general theory of geographic representation in GIS. *Int. J. GIS* **2007**, *21*, 239-260.
126. Cohen, J.M.; Ernst, K.C.; Lindblade, K.A.; Vulule, J.M.; John, C.C.; Wilson, M.L. Local topographic wetness indices predict household malaria risk better than land-use and land-cover in the western Kenya highlands. *Malaria J.* **2010**, *9*, 328.
127. Navulur, K. *Multispectral Image Analysis Using the Object-Oriented Paradigm*; CRC Press: Boca Raton, FL, USA, 2007; p. 163.

128. ITT. *Visual Information Solutions ENVI Software*. Available online: www.ittvis.com/ENVI (accessed on 20 October 2011).
129. Visual Learning Systems Inc. *Feature Analyst 4.2 for ArcGIS: Reference Manual*; Visual Learning Systems Inc.: Missoula, MT, USA, 2008.
130. ERDAS Inc. *Automating Feature Extraction with IMAGINE Objective: White Paper*; ERDAS Inc.: Norcross, GA, USA, 2009.
131. Clark Labs. *IDRISI Focus Paper: Segmentation and Segment-Based Classification*; Clark Labs: Worcester, MA, USA, 2009.

© 2011 by the authors; licensee MDPI, Basel, Switzerland. This article is an open access article distributed under the terms and conditions of the Creative Commons Attribution license (<http://creativecommons.org/licenses/by/3.0/>).